

# A level set formulation for Willmore flow

M. Droske, M. Rumpf\*

June 2, 2004

## Abstract

A level set formulation of Willmore flow is derived using the gradient flow perspective. Starting from single embedded surfaces and the corresponding gradient flow, the metric is generalized to sets of level set surfaces using the identification of normal velocities and variations of the level set function in time via the level set equation. The approach in particular allows to identify the natural dependent quantities of the derived variational formulation. Furthermore, spatial and temporal discretization are discussed and some numerical simulations are presented.

**AMS Subject Classifications:** 35K55, 53C44, 65M60, 74S05

## 1 Introduction

Let  $\mathcal{M}$  be a  $d$ -dimensional surface embedded in  $\mathbb{R}^{d+1}$  and denote by  $x$  the identity map on  $\mathcal{M}$ . Consider the energy

$$e[\mathcal{M}] := \frac{1}{2} \int_{\mathcal{M}} h^2 \, dA$$

where  $h$  is the mean curvature on  $\mathcal{M}$ , i. e.,  $h$  is the sum of the principle curvatures on  $\mathcal{M}$ . The corresponding  $L^2$ -gradient flow – the Willmore flow – is given by the geometric evolution problem [34, 32, 21]

$$\partial_t x(t) = \Delta_{\mathcal{M}(t)} h(t) n(t) + h(t) (\|S(t)\|_2^2 - \frac{1}{2} h(t)^2) n(t),$$

which defines for a given initial surface  $\mathcal{M}_0$  a family of surfaces  $\mathcal{M}(t)$  for  $t \geq 0$  with  $\mathcal{M}(0) = \mathcal{M}_0$ . Here  $S(t)$  denotes the shape operator on  $\mathcal{M}(t)$ ,  $n(t)$  the normal field on  $\mathcal{M}(t)$ , and  $\|\cdot\|_2$  the Frobenius norm on the space of endomorphisms on the tangent bundle  $\mathcal{T}\mathcal{M}(t)$ .

Now we consider  $\mathcal{M}(t)$  to be given implicitly as a specific level set of a corresponding function  $\phi(t) : \Omega \rightarrow \mathbb{R}$  for a domain  $\Omega \subset \mathbb{R}^{d+1}$ . Thus, the evolution of  $\mathcal{M}(t)$  can be described by an evolution of  $\phi(t)$ . In our case, the level set equation  $\partial_t \phi(t) +$

---

\*Numerical Analysis and Scientific Computing, Lotharstr. 65, University of Duisburg, 47057 Duisburg, Germany. e-mail: {droske, rumpf}@math.uni-duisburg.de

$\|\nabla\phi(t)\| V = 0$  (cf. the book of Osher and Paragios [25] for a detailed study), with  $V$  being the speed of propagation of the level set of  $\phi(t)$ , turns into the equation

$$\partial_t\phi + \|\nabla\phi(t)\| \left( \Delta_{\mathcal{M}}h + h(t) (\|S(t)\|_2^2 - \frac{1}{2}h(t)^2) \right) = 0, \quad (1)$$

with initial data  $\phi(0) = \phi_0$ . Here  $\phi_0$  implicitly describes the initial level set  $\mathcal{M}_0$ .

Let us emphasize that different from second order geometric evolution problems, such as mean curvature motion, for fourth order problems no maximum principle is known. Indeed, two surfaces both undergoing an evolution by Willmore flow may intersect in finite time. Hence, a level set formulation in general will lead to singularities and we expect a blow up of the gradient of  $\phi$  in finite time. If one is solely interested in the evolution of a single level set, one presumably can overcome this problem by a reinitialization with a signed distance function with respect to this evolving level set.

We are now aiming to derive a suitable weak formulation for the above evolution problem, which only makes use of first derivatives of unknown functions and test functions. This will in particular allow for a discretization based on a mixed formulation with piecewise affine finite elements, closely related to results by Rusu [28] for parametric Willmore flow.

Hence, we have to reformulate this problem solely in terms of quantities such as  $\phi(t)$ ,  $h(t)$  and its gradients, in particular avoiding the term  $\|S(t)\|_2$  and derivatives of the normal. Here, we take advantage of a fairly general gradient flow perspective to geometric evolution problems. Indeed, given a gradient flow for parametric surfaces we derive in Section 3 a level set formulation which describes the simultaneous evolution of all level sets corresponding to this gradient flow. This approach is based on the co-area formula (cf. for example to the book of Ambrosio et al. [1]) and a proper identification of the temporal change of the level set function and the corresponding evolution speed of the level surfaces. Thereby, we are able to identify the natural dependent variables. This approach gives insight in the geometry of evolution problems on the space of level set ensembles. We apply it for Willmore flow in Section 4 and outline the correspondence to a spatial integration of the well known gradient of the parametric Willmore functional in Section 5. Here, we confine to a formal analysis and do not discuss questions concerning well-posedness, short or long time existence and regularity. Indeed, there is not very much known so far (see below). Boundary conditions are discussed in Section 7 and a suitable regularization taking care of degenerate gradients  $\nabla\phi = 0$  and being related to Willmore flow for graphs is introduced in Section 6. Besides the derivation of the weak formulation we deduce a mixed semiimplicit finite element discretization in Section 8 and show some numerical results.

Concerning physical modeling the minimization of the Willmore energy is closely related to the minimization of the bending energy of an elastic shell (cf. the monograph of Ciarlet [9] and the shell simulation by Schroeder et al.[20, 19]). A further potential application of Willmore flow is in image processing and related to image inpainting or restoration of implicit surfaces. Methods based on similar ideas can be found in the works of Kobbelt and Schneider [29, 30] and Yoshizawa and Belayev[35]. In the restoration of flat 2D images – known as the inpainting problem – variational methods have proved to be successful tools. Here, higher order methods were presented for

instance by Bertalmio et al. [7, 6]. The normal directions on level sets and the grey values are prescribed at the boundary of the inpainting domain and an energy depending on directions and image intensities is then minimized under these boundary conditions, subject to the constraint that the directions are perpendicular on the level sets of the corresponding image intensity field.

Furthermore, curvature based inpainting methods have been proposed by Masnou, Morel [24, 2] and Chan et al. [8]. They treat the level sets of a 2D images as Euler's elastica and minimize their bending energy. In particular Ambrosio and Masnou proved existence of minimizers of the Willmore energy in the level set context [2] making extensive use of techniques from geometric measure theory.

Recently, the  $L^2$ -gradient flow of the Willmore energy was considered analytically. Simonett [32] was able to prove long time existence for surfaces close to spheres in the  $C^{2,\alpha}$  topology. Kuwert and Schätzle [22] show the existence of a lower bound on the maximal time for which smooth solutions for Willmore flow exist. In particular they analyze the concentration of curvature. In [21, 23] they are able to prove convergence to round spheres under suitable assumptions on the initial surface. The case of curves moving in space w.r.t. Willmore flow is treated in [16] together with Dziuk analytically as well as numerically. They generalize results of Polden for planar curves [26, 27] and give a semi-implicit discretization scheme. In [28] Rusu presented a new approach for a weak formulation for parametric Willmore flow which allows a mixed finite element discretization. In [10] this scheme has been generalized with respect to boundary conditions. Recently, Bänsch et al. [3, 4] presented a novel numerical algorithm for surface diffusion, which is the gradient flow of the area with respect to the  $H^{-1}$  metric. For a general overview on the numerical analysis of geometric evolution problems we refer to Deckelnick and Dziuk [11, 14, 13]. In [15] Deckelnick, Dziuk and Elliott discussed surface diffusion for axial symmetric surfaces.

## 2 Some useful geometric tools

At first, let us introduce some useful notation and derive representations for geometric quantities on level sets  $\mathcal{M}$  in terms of the corresponding level set function  $\phi$ . Let  $\phi : \Omega \rightarrow \mathbb{R}$  be some smooth function on a domain  $\Omega \subset \mathbb{R}^{d+1}$ . Suppose  $\mathcal{M}_c := \{x \in \Omega \mid \phi(x) = c\}$  is a level set of  $\phi$  for the level value  $c$ . For the sake of simplicity, we simply write  $\mathcal{M} = \mathcal{M}_c$  and assume that  $\|\nabla\phi\| \neq 0$  on  $\mathcal{M}$ . Hence by the implicit function theorem,  $\mathcal{M}_c$  is a smooth hypersurface and the normal

$$n = \frac{\nabla\phi}{\|\nabla\phi\|}$$

on the tangent space  $\mathcal{T}_x\mathcal{M}$  is defined for every  $x$  on  $\mathcal{M}$ . In what follows we will make extensive use of the Einstein summation convention. Furthermore vectors  $v \in \mathbb{R}^{d+1}$  and matrixes  $A \in \mathbb{R}^{d+1,d+1}$  are written in index form

$$v = (v_i)_i, \quad A = (A_{ij})_{ij}$$

Let us introduce some important differential operators based on *tangential differentiation*. For a tangential vector field  $v$  on  $\mathcal{M}$  and a scalar function  $u$  on  $\mathbb{R}^{d+1}$  we obtain

$$\begin{aligned}\operatorname{div}_{\mathcal{M}} v &= v_{i,i} - n_i n_j v_{i,j} \\ \nabla_{\mathcal{M}} u &= (u_{,i} - n_i n_j u_{,j})_i\end{aligned}$$

and we abbreviate in the usual way  $\partial_j u = u_{,j}$  and  $\partial_j v_i = v_{i,j}$ . As an exercise, let us compute the Laplace Beltrami operator with respect to a level set  $\mathcal{M}$  for a function  $u$  extended on the whole domain  $\Omega$

$$\begin{aligned}\Delta_{\mathcal{M}} u &= \operatorname{div}_{\mathcal{M}} \nabla_{\mathcal{M}} u \\ &= (\partial_i - n_i n_k \partial_k)(u_{,i} - n_i n_j u_{,j}) \\ &= u_{,ii} - n_i n_k u_{,ik} - h n_j u_{,j} - n_i n_j u_{,j,i} - n_i n_j u_{,ji} \\ &\quad + n_i n_k n_j u_{,jk} + n_i n_k n_i n_j u_{,j,i} + n_i n_k n_i n_j u_{,k,j} \\ &= u_{,ii} - n_i n_k u_{,ik} - h n_j u_{,j} \\ &= \Delta_{\mathbb{R}^{d+1}} u - h \partial_n u - \partial_n^2 u,\end{aligned}\tag{2}$$

and thereby retrieve a classical result. Here, we have used  $0 = \partial_j \|n\|^2 = 2n_i n_{i,j}$  and the fact that  $h := \operatorname{div} n = n_{i,i}$  is the mean curvature on  $\mathcal{M}$ . Next, let us consider the shape operator on implicit surfaces. We evaluate the Jacobian of the normal field

$$Dn = \frac{1}{\|\nabla\phi\|} \left( \phi_{,ij} - \frac{\phi_{,i}}{\|\nabla\phi\|} \frac{\phi_{,k}}{\|\nabla\phi\|} \phi_{,kj} \right)_{ij} = \frac{1}{\|\nabla\phi\|} P D^2 \phi\tag{3}$$

where  $P = (\delta_{ij} - n_i n_j)_{ij} = \mathbb{I} - n \otimes n$  is the projection on the tangent space and  $\mathbb{I}$  indicates the identity mapping. In particular,  $P = P^T = P^2$  holds. Hence, for the shape operator  $S$  (which is the restriction of  $Dn$  on the tangent space) we obtain

$$S = Dn P = \frac{1}{\|\nabla\phi\|} P D^2 \phi P.\tag{4}$$

Finally, let us consider the Frobenius norm  $\|A\|_2 = \sqrt{A : A}$  for the shape operator  $S$ , where  $A : B = \operatorname{tr}(A^T B) = A_{ij} B_{ij}$  for  $A, B \in \mathbb{R}^{d+1, d+1}$ . We obtain

$$\begin{aligned}\|S\|^2 &= \operatorname{tr}(S^T S) = \frac{1}{\|\nabla\phi\|^2} \operatorname{tr}(P D^2 \phi P P D^2 \phi P) \\ &= \frac{1}{\|\nabla\phi\|^2} \operatorname{tr}(P D^2 \phi P D^2 \phi P) = \frac{1}{\|\nabla\phi\|^2} \operatorname{tr}(P D^2 \phi P P D^2 \phi) \\ &= \frac{1}{\|\nabla\phi\|^2} \operatorname{tr}(P D^2 \phi P D^2 \phi) = \operatorname{tr}(Dn Dn) = Dn^T : Dn.\end{aligned}\tag{5}$$

### 3 The gradient flow perspective

Given a general energy density  $f$  on a surface  $\mathcal{M}$

$$e[\mathcal{M}] := \int_{\mathcal{M}} f \, dA$$

we consider the gradient flow with respect to the  $L^2$  surface metric

$$\partial_t x = -\text{grad}_{L^2(\mathcal{M})} e[\mathcal{M}],$$

where the  $L^2$  metric on  $\mathcal{M}$  is given by

$$g_{\mathcal{M}}(v_1, v_2) = \int_{\mathcal{M}} v_1 v_2 \, dA$$

for two scalar, normal velocities  $v_1, v_2$  on  $\mathcal{M}$ . Let us assume that we simultaneously want to evolve all level sets  $\mathcal{M}_c$  of a given level set function  $\phi$ . Hence, we take into account the co-area formula [18, 1] to define a global energy

$$E[\phi] := \int_{\mathbb{R}} e[\mathcal{M}_c] \, dc = \int_{\Omega} \|\nabla\phi\| f \, dx,$$

where we set  $e[\mathcal{M}_c] = 0$  if  $\mathcal{M}_c = \emptyset$ . We interpret a function  $\phi$  and thus the set of level sets  $\{\mathcal{M}_c\}_{c \in \mathbb{R}}$  as an element of the manifold  $\mathcal{L}$  of level set ensembles which carries a trivial linear structure, because we so far do not impose any constraints. A tangent vector  $s := \partial_t \phi$  on  $\mathcal{L}$  can be identified with a motion velocity  $v$  of the level sets  $\mathcal{M}_c$  via the classical level set equation:

$$s + \|\nabla\phi\| v = 0. \quad (6)$$

Thus, we are able to define a metric on  $\mathcal{L}$

$$\begin{aligned} g_{\phi}(s_1, s_2) &:= \int_{\mathbb{R}} g_{\mathcal{M}_c}(v_1, v_2) \, dc = \int_{\mathbb{R}} \int_{\mathcal{M}_c} v_1 v_2 \, dA \, dc \\ &= \int_{\Omega} \frac{s_1}{\|\nabla\phi\|} \frac{s_2}{\|\nabla\phi\|} \|\nabla\phi\| \, dx = \int_{\Omega} s_1 s_2 \|\nabla\phi\|^{-1} \, dx \end{aligned}$$

for two tangent vectors  $s_1, s_2$  with corresponding normal velocities  $v_1, v_2$ . Finally, we are able to rewrite the simultaneous gradient flow of all level sets in terms of the level set function  $\phi$

$$\partial_t \phi = -\text{grad}_{g_{\phi}} E[\phi],$$

which is equivalent to

$$g_{\phi}(\partial_t \phi, \vartheta) = \int_{\Omega} \partial_t \phi \vartheta \|\nabla\phi\|^{-1} \, dx = -\langle E'[\phi], \vartheta \rangle \quad (7)$$

for all functions  $\vartheta \in C_0^{\infty}(\Omega)$ . Let us emphasize that the velocity  $\vartheta$  has to be interpreted as a tangent vector on  $\mathcal{L}$ .

As an example let us first consider  $e[\mathcal{M}] = \text{area}(\mathcal{M})$  with  $f = 1$ . Hence,  $E[\phi] = \int_{\Omega} \|\nabla\phi\|$  and we obtain the evolution equation

$$\int_{\Omega} \partial_t \phi \vartheta \|\nabla\phi\|^{-1} \, dx = - \int_{\Omega} \frac{\nabla\phi}{\|\nabla\phi\|} \cdot \nabla\vartheta \, dx.$$

Indeed, this is the weak formulation of mean curvature motion in level set form (cf. Evans and Spruck [17] as well as Deckelnick and Dziuk [11]).

## 4 Willmore flow in level set form

Next, we proceed with the equation for Willmore flow and consider the energy

$$e[\mathcal{M}] = \frac{1}{2} \int_{\mathcal{M}} h^2 \, dA$$

As simultaneous version of the gradient flow  $\partial_t x = -\text{grad}_{L^2(\mathcal{M})} e[\mathcal{M}]$  for all level sets we obtain the evolution problem

$$\partial_t \phi = -\text{grad}_{g_\phi} E[\phi]$$

on  $\mathcal{L}$  and evaluate

$$\begin{aligned} \int_{\Omega} \frac{\partial_t \phi \vartheta}{\|\nabla \phi\|} \, dx &= - \frac{d}{d\epsilon} E[\phi + \epsilon \vartheta] \Big|_{\epsilon=0} \\ &= - \frac{d}{d\epsilon} \frac{1}{2} \int_{\Omega} \|\nabla(\phi + \epsilon \vartheta)\| \left( \text{div} \left[ \frac{\nabla(\phi + \epsilon \vartheta)}{\|\nabla(\phi + \epsilon \vartheta)\|} \right] \right)^2 \, dx \Big|_{\epsilon=0} \\ &= - \int_{\Omega} \frac{1}{2} h^2 \frac{\nabla \phi}{\|\nabla \phi\|} \cdot \nabla \vartheta + \|\nabla \phi\| \, h \, \text{div} \left[ \frac{d}{d\epsilon} n_{\phi + \epsilon \vartheta} \Big|_{\epsilon=0} \right] \, dx \\ &= - \int_{\Omega} \frac{1}{2} h^2 \frac{\nabla \phi}{\|\nabla \phi\|} \cdot \nabla \vartheta + \|\nabla \phi\| \, h \, \text{div} \left[ \|\nabla \phi\|^{-1} P \nabla \vartheta \right] \, dx \\ &= \int_{\Omega} -\frac{1}{2} \|\nabla \phi\|^{-3} (\|\nabla \phi\| \, h)^2 \nabla \phi \cdot \nabla \vartheta + \\ &\quad \|\nabla \phi\|^{-1} P \nabla (\|\nabla \phi\| \, h) \cdot \nabla \vartheta \, dx . \end{aligned} \tag{8}$$

Here, we have used the notation

$$n_\phi := \frac{\nabla \phi}{\|\nabla \phi\|}$$

and the variational formula

$$\begin{aligned} \frac{d}{d\epsilon} n_{\phi + \epsilon \vartheta} \Big|_{\epsilon=0} &= \frac{\nabla \vartheta}{\|\nabla \phi\|} - \frac{\nabla \phi}{\|\nabla \phi\|^2} \frac{\nabla \phi}{\|\nabla \phi\|} \cdot \nabla \vartheta \\ &= \|\nabla \phi\|^{-1} P \nabla \vartheta . \end{aligned}$$

It turns out that the weighed mean curvature

$$w := -\|\nabla \phi\| \, h$$

– to be understood as a curvature concentration – is the natural dependent quantity arising in a weak formulation of the evolution problem. For  $w$  we obtain the equation

$$\int_{\Omega} \|\nabla \phi\|^{-1} w \, \psi \, dx = \int_{\Omega} \frac{\nabla \phi}{\|\nabla \phi\|} \cdot \nabla \psi \, dx$$

for all  $\psi \in C_0^\infty(\Omega)$ . Finally, we end up with the following initial value problem for Willmore flow in level set form:

Given an initial function  $\phi_0$  on  $\Omega$  find a pair of functions  $(\phi, w)$  with  $\phi(0) = \phi_0$ , such that

$$\int_{\Omega} \frac{\partial_t \phi}{\|\nabla \phi\|} \vartheta \, dx = \int_{\Omega} -\frac{1}{2} \frac{w^2}{\|\nabla \phi\|^3} \nabla \phi \cdot \nabla \vartheta - \|\nabla \phi\|^{-1} P \nabla w \cdot \nabla \vartheta \, dx, \quad (9)$$

$$\int_{\Omega} \|\nabla \phi\|^{-1} w \psi \, dx = \int_{\Omega} \frac{\nabla \phi}{\|\nabla \phi\|} \cdot \nabla \psi \, dx \quad (10)$$

for all  $t > 0$  and all functions  $\vartheta, \psi \in C_0^\infty(\Omega)$ .

## 5 Cross checking the evolution equation

Another approach to derive a level set formulation for Willmore flow consists in transforming the well known parametric gradient flow formulation appropriately and derive from it by straightforward computation a weak formulation. We find it instructive to cross check our above result (8) and in particular to underline that the gradient flow perspective is more intuitive.

Multiplying (1) with the test function  $\vartheta \|\nabla \phi(t)\|^{-1}$  for arbitrary  $\vartheta \in C_0^\infty(\Omega)$  and integrating over  $\Omega$  one obtains

$$\int_{\Omega} \frac{\partial_t \phi(t)}{\|\nabla \phi(t)\|} \vartheta + \Delta_{\mathcal{M}} h(t) \vartheta + h(t) (\|S(t)\|_2^2 - \frac{1}{2} h(t)^2) \vartheta \, dx = 0.$$

At first, we recall from above that  $\|S(t)\|^2 = Dn^T : Dn$  and  $h = \operatorname{div} n$ . Thus, applying (2) we obtain

$$\begin{aligned} \int_{\Omega} \Delta_{\mathcal{M}} h \vartheta \, dx &= \int_{\Omega} \Delta h \vartheta - h n_i h_{,i} \vartheta - h_{,ij} n_i n_j \vartheta \, dx \\ &= \int_{\Omega} -\nabla h \nabla \vartheta - \frac{1}{2} n_i (h^2)_{,i} \vartheta - h_{,ij} n_i n_j \vartheta \, dx \\ &= \int_{\Omega} -\nabla h \nabla \vartheta - \frac{1}{2} n_i (h^2)_{,i} \vartheta + h_{,j} n_i n_j \vartheta_{,i} + \frac{1}{2} (h^2)_{,j} n_j \vartheta + h_{,j} n_i n_{j,i} \vartheta \, dx \\ &= \int_{\Omega} -P \nabla h \nabla \vartheta + h_{,j} n_i n_{j,i} \vartheta \, dx. \end{aligned}$$

Furthermore, again using integration by parts we observe

$$\begin{aligned} \int_{\Omega} h \|S\|^2 \vartheta \, dx &= \int_{\Omega} h n_{j,i} n_{i,j} \vartheta \, dx \\ &= \int_{\Omega} -h_{,i} n_j n_{i,j} \vartheta - h n_j n_{i,j,i} \vartheta - h n_j n_{i,j} \vartheta_{,i} \, dx \\ &= \int_{\Omega} -h_{,i} n_j n_{i,j} \vartheta - \frac{1}{2} (h^2)_{,j} n_j \vartheta - h n_j n_{i,j} \vartheta_{,i} \, dx \end{aligned}$$

and finally

$$- \int_{\Omega} \frac{1}{2} h h^2 \vartheta \, dx = - \int_{\Omega} \frac{1}{2} h^2 n_{j,j} \vartheta \, dx = \int_{\Omega} \frac{1}{2} (h^2)_{,j} n_j \vartheta + \frac{1}{2} h^2 n_{j,j} \vartheta \, dx.$$

Collecting all these terms we end up with

$$\begin{aligned} & \int_{\Omega} \Delta_{\mathcal{M}} h + h (\|S\|^2 - \frac{1}{2} h^2) \vartheta \, dx = \int_{\Omega} -P \nabla h \nabla \vartheta - h n_j n_{i,j} \vartheta_{,i} + \frac{1}{2} h^2 n_{j,j} \vartheta \, dx \\ & = \int_{\Omega} -P \nabla h \nabla \vartheta - \frac{h}{\|\nabla \phi\|} P \nabla (\|\nabla \phi\|) \cdot \nabla \vartheta + \frac{1}{2} h^2 n \cdot \nabla \vartheta \, dx \\ & = \int_{\Omega} -\|\nabla \phi\|^{-1} P \nabla (\|\nabla \phi\| h) \cdot \nabla \vartheta + \frac{1}{2} \|\nabla \phi\|^{-3} (\|\nabla \phi\| h)^2 \nabla \phi \cdot \nabla \vartheta \, dx, \end{aligned}$$

where we have used that (3) implies

$$Dn n = \frac{1}{\|\nabla \phi\|} P D^2 \phi n = \frac{1}{\|\nabla \phi\|} P \nabla (\|\nabla \phi\|).$$

Thus, we have verified that the level set equations (8) derived from the gradient flow perspective coincides with the evolution problem deduced from a straightforward integration of the gradient of the parametric Willmore energy.

## 6 Regularization and graph surfaces

Before we start discretizing the evolution problem (9), (10) let us introduce a suitable regularization to avoid singularities in case of a vanishing gradient  $\|\nabla \phi\|$  of the level set function. We introduce  $\|v\|_{\epsilon} := (\|v\|^2 + \epsilon)^{\frac{1}{2}}$  for  $v \in \mathbb{R}^d$  and replace all occurrences of  $\|\nabla \phi\|$  in (9) and (10) by  $\|\nabla \phi\|_{\epsilon}$ . Similar to many other geometric evolution problems [14, 12], regularized Willmore flow can be interpreted as the corresponding flow of scaled graphs in  $\mathbb{R}^{d+2}$ . Indeed, for a given function  $\phi : \Omega \mapsto \mathbb{R}$  let us consider the graph

$$\mathcal{G}^{\epsilon} = \{(x, \epsilon^{-1} \phi(x)) \mid x \in \Omega\}.$$

We denote by  $n^{\epsilon} := \|(-\nabla \phi, \epsilon)^T\|^{-1} (-\nabla \phi, \epsilon)^T$  the upward oriented normal on the graph  $\mathcal{G}^{\epsilon}$ . By

$$g_{\phi, \epsilon}(s_1, s_2) := g_{\mathcal{G}^{\epsilon}}(v_1^{\epsilon}, v_2^{\epsilon}) = \int_{\mathcal{G}^{\epsilon}} v_1^{\epsilon} v_2^{\epsilon} \, dA$$

we define the natural metric on normal bundles on  $\mathcal{G}^{\epsilon}$ , where  $v_1^{\epsilon}, v_2^{\epsilon}$  are scalar normal velocities of the evolving graph in direction  $n^{\epsilon}$ . Any velocity  $v^{\epsilon}$  in this graph normal direction  $n^{\epsilon}$  corresponds to a velocity  $v$  of the corresponding level set in direction of the level set normal  $n$ , in particular

$$v^{\epsilon} = -v \frac{\|\nabla \phi\|}{\|\nabla \phi\|_{\epsilon}}. \quad (11)$$



Indeed, observe that  $\cos \alpha = \|\nabla \phi\| \|\nabla \phi\|_\epsilon^{-1}$  holds for the angle  $\alpha$  between  $n^\epsilon$  and the normal  $-n$  on the level set in the  $\mathbb{R}^{d+1}$  plane. Using the identification (11) and (6) we can rewrite the metric

$$\begin{aligned} g_{\phi,\epsilon}(s_1, s_2) &= \int_{\Omega} \sqrt{1 + \epsilon^{-2} \|\nabla \phi\|^2} v_1^\epsilon v_2^\epsilon \, dx \\ &= \int_{\Omega} \frac{\|\nabla \phi\|_\epsilon}{\epsilon} v_1 v_2 \frac{\|\nabla \phi\|^2}{\|\nabla \phi\|_\epsilon^2} \, dx \\ &= \frac{1}{\epsilon} \int_{\Omega} \frac{s_1 s_2}{\|\nabla \phi\|_\epsilon} \, dx. \end{aligned}$$

On the other hand, the Willmore energy  $e[\mathcal{G}^\epsilon]$  of the graph surface  $\mathcal{G}^\epsilon$  is given by

$$\begin{aligned} e[\mathcal{G}^\epsilon] &= \int_{\mathcal{G}^\epsilon} (h^\epsilon)^2 \, dA \\ &= \int_{\Omega} \sqrt{1 + \epsilon^{-2} \|\nabla \phi\|^2} \left( \operatorname{div} \left[ \frac{\epsilon^{-1} \nabla \phi}{\sqrt{1 + \epsilon^{-2} \|\nabla \phi\|^2}} \right] \right)^2 \, dx \\ &= \frac{1}{\epsilon} \int_{\Omega} \|\nabla \phi\|_\epsilon \left( \operatorname{div} \left[ \frac{\nabla \phi}{\|\nabla \phi\|_\epsilon} \right] \right)^2 \, dx \\ &=: \epsilon^{-1} E_\epsilon[\phi], \end{aligned}$$

where  $h^\epsilon$  is the mean curvature of the  $d + 1$  dimensional graph surface  $\mathcal{G}^\epsilon$  and  $E_\epsilon[\phi]$  turns out to be the regularized version of the Willmore energy. Hence, the regularized gradient flow

$$g_{\phi,\epsilon}(\partial_t \phi, \vartheta) = -\langle E'_\epsilon[\phi], \vartheta \rangle$$

can be understood as an approximation of the actual Willmore flow (7) for implicit surfaces via a Willmore flow for graph surfaces with a scaling  $\epsilon^{-1}$  for  $\epsilon \rightarrow \infty$  (cf. [17]).

## 7 Boundary conditions

So far, we have not imposed any boundary conditions on  $\partial\Omega$ . We might allow for test functions  $\vartheta, \psi \in C^\infty(\Omega)$ . Then, assuming sufficient regularity for the solution  $(\phi, w)$  and applying integration by parts in equation (10), we obtain by the fundamental lemma the differential equation  $h = -\|\nabla \phi\|^{-1} w = \operatorname{div} \frac{\nabla \phi}{\|\nabla \phi\|}$  in  $\Omega$  and the boundary condition  $\frac{\nabla \phi}{\|\nabla \phi\|} \cdot \nu = 0$  on  $\partial\Omega$ . Here  $\nu$  denotes the outer normal on  $\partial\Omega$ . Hence, the level sets are orthogonal on  $\partial\Omega$ . Furthermore, applying integration by parts also in equation (9), we obtain

$$\partial_t \phi - \|\nabla \phi\| \operatorname{div} \left( \frac{h^2}{2} \frac{\nabla \phi}{\|\nabla \phi\|} + \|\nabla \phi\|^{-1} P \nabla w \right) = 0 \quad \text{in } \Omega$$

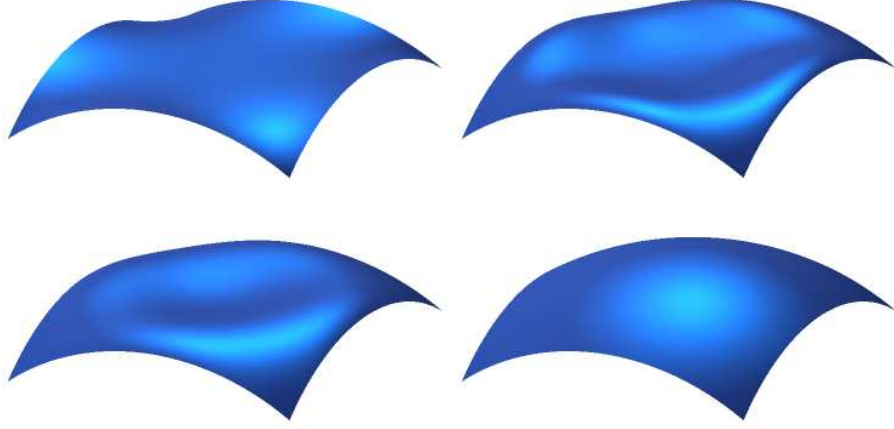


Figure 1: Given an initial graph (upper left) Willmore flow with prescribed Dirichlet boundary conditions for the position and the normal is applied. Different timesteps of the evolution (from left to right and from top to bottom) are displayed. The boundary condition corresponds to a spherical cap over the graph domain which is reflected by the limit surface (lower right) for  $t \rightarrow \infty$ .

and on  $\partial\Omega$  we get  $\frac{h^2}{2} \frac{\nabla\phi}{\|\nabla\phi\|} \cdot \nu + \|\nabla\phi\|^{-1} P\nabla w \cdot \nu = 0$ . From  $\frac{\nabla\phi}{\|\nabla\phi\|} \perp \nu$  we deduce that  $P\nu = \nu$  and end up with the second boundary condition  $\nabla w \cdot \nu = 0$ .

Alternatively, we might consider test functions  $\vartheta \in C_0^\infty(\Omega)$  and  $\psi \in C^\infty(\Omega)$  and replace equation (10) by

$$\int_{\Omega} \|\nabla\phi\|^{-1} w \psi \, dx = \int_{\Omega} \frac{\nabla\phi}{\|\nabla\phi\|} \cdot \nabla\psi \, dx - \int_{\partial\Omega} \gamma \psi \, dA, \quad (12)$$

for some scalar function  $\gamma$  on  $\partial\Omega$ , with  $|\gamma| \leq 1$ . Then, we obtain the same differential equations in  $\Omega$  and the boundary condition  $n \cdot \nu = \gamma$  on  $\partial\Omega$ . Hence, we are able to impose  $\phi = \phi^\partial$  for some function  $\phi^\partial$  on  $\partial\Omega$  and to enforce a boundary conditions  $n = n^\partial$  for  $n = \frac{\nabla\phi}{\|\nabla\phi\|}$  and some normal field  $n^\partial$  on  $\partial\Omega$ . Indeed, the tangential component  $(\mathbb{I} - \nu \otimes \nu)n$  is already uniquely determined by  $\phi^\partial$ . We obtain,

$$\begin{aligned} n^\partial &= (\mathbb{I} - \nu \otimes \nu)n + \gamma\nu = \frac{(\mathbb{I} - \nu \otimes \nu)\phi + \gamma\|\nabla\phi\|\nu}{\|(\mathbb{I} - \nu \otimes \nu)\phi + \gamma\|\nabla\phi\|\nu\|} \\ &= \frac{\nabla_{\partial\Omega}\phi^\partial + \gamma\beta\nu}{\|\nabla_{\partial\Omega}\phi^\partial + \gamma\beta\nu\|}, \end{aligned}$$

where  $\beta := \|\nabla\phi\| = (1 - \gamma^2)^{-\frac{1}{2}} \|\nabla_{\partial\Omega}\phi\|$  and  $\nabla_{\partial\Omega}$  denotes the tangential gradient on  $\partial\Omega$ . For consistency purposes we have to set  $|\gamma| = 1$  if  $\nabla_{\partial\Omega}\phi^\partial = 0$ .

In case of Willmore flow for graphs as discussed in Section 6 we can proceed analogously to impose  $C^1$  boundary conditions on  $\partial\Omega$  and replace the graph version of

equation (10) by

$$\int_{\Omega} \|\nabla\phi\|_{\epsilon}^{-1} w \psi \, dx = \int_{\Omega} \frac{\nabla\phi}{\|\nabla\phi\|_{\epsilon}} \cdot \nabla\psi \, dx - \int_{\partial\Omega} \gamma\psi \, dA, \quad (13)$$

for some function  $\gamma$  on  $\partial\Omega$  with  $|\gamma| < 1$ . Applying integration by parts we obtain the differential equation in  $\Omega$  and on  $\partial\Omega$  the boundary condition

$$\frac{\nabla\phi}{\|\nabla\phi\|_{\epsilon}} \cdot \nu = \gamma.$$

Again, we can decompose  $\nabla\phi$  and get  $\nabla\phi = (\mathbb{I} - \nu \otimes \nu)\nabla\phi + \gamma \|\nabla\phi\|_{\epsilon} \nu$ , where the tangential component  $(\mathbb{I} - \nu \otimes \nu)\nabla\phi$  as above only depends on  $\phi^{\partial}$ . In analogy to our preceding derivation, we set  $\beta := \|\nabla\phi\|_{\epsilon} = (1 - \gamma^2)^{-\frac{1}{2}} \|\nabla_{\partial\Omega}\phi^{\partial}\|_{\epsilon}$  and obtain for the graph normal  $n^{\epsilon, \partial}$  on  $\partial\Omega$

$$n^{\epsilon, \partial} = \frac{(-\nabla_{\partial\Omega}\phi^{\partial} - \gamma\beta\nu, \epsilon)^T}{\|\nabla_{\partial\Omega}\phi^{\partial} + \gamma\beta\nu\|_{\epsilon}}.$$

## 8 A semiimplicit finite element discretization

Now we proceed with the temporal and spatial discretization of the regularized Willmore flow problem. We discretize the system of partial differential equations (9), (10) first in space using piecewise affine finite elements and then in time based on a semi implicit backward Euler scheme.

*Spatial discretization.* Let us consider a uniform rectangular ( $d = 1$ ) or hexahedral ( $d = 2$ ) mesh  $\mathcal{C}$  covering the whole image domain  $\Omega$  and consider the corresponding bilinear respectively trilinear interpolation on cells  $C \in \mathcal{C}$  to obtain discrete intensity functions in the accompanying finite element space  $V^h$ . Here, the superscript  $h$  indicates the grid size. Suppose  $\{\Phi_i\}_{i \in I}$  is the standard basis of hat shaped base functions corresponding to nodes of the mesh indexed over an index set  $I$ . To clarify the notation we will denote spatially discrete quantities with upper case letters to distinguish them from the corresponding continuous quantities in lower case letters. Hence, we obtain

$$V^h = \{\Phi \in C^0(\Omega) \mid \Phi|_C \in \mathcal{P}_1 \forall C \in \mathcal{C}\},$$

where  $\mathcal{P}_1$  denotes the space of  $(d + 1)$ -linear (bilinear or trilinear) functions. Suppose  $\mathcal{I}_h$  is the Lagrangian interpolation onto  $V^h$ . Now, we formulate the semi discrete finite element problem:

*Find a function  $\Phi : \mathbb{R}_0^+ \rightarrow V^h$  with  $\Phi(0) = \mathcal{I}_h\phi_0$  and a corresponding mean curvature function  $W : \mathbb{R}^+ \rightarrow V^h$ , such that*

$$\begin{aligned} \int_{\Omega} \frac{\partial_t \Phi(t)}{\|\nabla\Phi(t)\|} \Theta \, dx &= \int_{\Omega} -\frac{W(t)^2}{2\|\nabla\Phi(t)\|^3} \nabla\Phi(t) \cdot \nabla\Theta - \frac{P_{\epsilon}[\Phi(t)]}{\|\nabla\Phi(t)\|} \nabla W(t) \cdot \nabla\Theta \, dx \\ \int_{\Omega} \frac{W(t)}{\|\nabla\Phi(t)\|} \Psi \, dx &= \int_{\Omega} \frac{\nabla\Phi(t)}{\|\nabla\Phi(t)\|} \cdot \nabla\Psi \, dx \end{aligned}$$

for all  $t > 0$  and all test functions  $\Theta, \Psi \in V^h$ . Here, we use the notation

$$P_\epsilon[\Phi^k] = \left( \mathbb{I} - \frac{\nabla\Phi}{\|\nabla\Phi\|_\epsilon} \otimes \frac{\nabla\Phi}{\|\nabla\Phi\|_\epsilon} \right)$$

and consider Neumann boundary conditions on  $\partial\Omega$ .

*Time discretization.* Furthermore, for a given time step  $\tau > 0$  we aim to compute discrete functions  $\Phi^k(\cdot) \in V^h$ , which approximate  $\phi(k\tau, \cdot)$  on  $\Omega$ . Thus, we replace the time derivative  $\partial_t\phi$  by a backward difference quotient and evaluate all terms related to the metric on the previous time step. In particular in the  $(k+1)$ th time step the weight  $\|\nabla\Phi\|$  and the projection  $P$  are taken from the  $k$ th time step. Explicit time discretizations are ruled out due to accompanying severe time step restrictions of the type  $\tau \leq C(\epsilon)h^4$ , where  $h$  is the spatial grid size (cf. results presented in [35, 8]). We are left to decide, which terms in each time step to consider explicitly and which implicitly. We present here two variants, which turn out to behave equally well in our numerical experiments concerning stability.

**Variant I.**

Find a sequence of image intensity functions  $(\Phi^k)_{k=0,\dots} \subset V^h$  with  $\Phi^0 = \mathcal{I}_h\phi_0$  and a corresponding sequence of functions of mean curvature concentration  $(W^k)_{k=0,\dots} \subset V^h$  such that

$$\begin{aligned} \int_{\Omega} \frac{\Phi^{k+1} - \Phi^k}{\tau \|\nabla\Phi^k\|_\epsilon} \Theta + \frac{P_\epsilon[\Phi^k]}{\|\nabla\Phi^k\|_\epsilon} \nabla W^{k+1} \cdot \nabla \Theta \, dx &= \int_{\Omega} \frac{-(W^k)^2}{2\|\nabla\Phi^k\|_\epsilon^3} \nabla\Phi^{k+1} \cdot \nabla \Theta \, dx \\ \int_{\Omega} \frac{W^{k+1}}{\|\nabla\Phi^k\|_\epsilon} \Psi \, dx &= \int_{\Omega} \frac{\nabla\Phi^{k+1}}{\|\nabla\Phi^k\|_\epsilon} \cdot \nabla \Psi \, dx \end{aligned}$$

for all test functions  $\Theta, \Psi \in V^h$ .

**Variant II.**

Find a sequence of image intensity functions  $(\Phi^k)_{k=0,\dots} \subset V^h$  with  $\Phi^0 = \mathcal{I}_h\phi_0$  and a corresponding sequence of functions of mean curvature concentration  $(W^k)_{k=0,\dots} \subset V^h$  such that

$$\begin{aligned} \int_{\Omega} \frac{\Phi^{k+1} - \Phi^k}{\tau \|\nabla\Phi^k\|_\epsilon} \Theta + \frac{\nabla W^{k+1}}{\|\nabla\phi^k\|_\epsilon} \cdot \nabla \Theta \, dx &= \int_{\Omega} -\frac{(W^k)^2}{2\|\nabla\Phi^k\|_\epsilon^3} \nabla\Phi^{k+1} \cdot \nabla \Theta \\ &\quad + \frac{(\mathbb{I} - P_\epsilon[\Phi^k])}{\|\nabla\Phi^k\|_\epsilon} \nabla W^k \cdot \nabla \Theta \, dx \\ \int_{\Omega} \frac{W^{k+1}}{\|\nabla\Phi^k\|_\epsilon} \Psi \, dx &= \int_{\Omega} \frac{\nabla\Phi^{k+1}}{\|\nabla\Phi^k\|_\epsilon} \cdot \nabla \Psi \, dx \end{aligned}$$

for all test functions  $\Theta, \Psi \in V^h$ .

**Remark:** As we have discussed in Section 4 the first term on the right hand side of the evolution equation for  $\phi$  represents the discrete variation of the weight  $\|\nabla\phi\|$  for fixed energy integrand  $h^2$ , whereas the second term reflects the variation of the energy integrand  $h^2$  for fixed weight  $\|\nabla\phi\|$ . The first term is primarily of second order,

whereas the second one is of fourth order. Nevertheless, our numerical experiments pointed out that it is essential to consider the first term implicitly as well. Otherwise, we observe instabilities and correspondingly more restrictive time step constraints (cf. [10]).

To obtain a fully preactival finite element method, we consider numerical quadrature. We replace the parabolic term and the left hand side of the second equation using standard mass lumping [33]. For the other terms we apply a lower order Gaussian quadrature rule. In particular, we introduce the piecewise constant projection  $\mathcal{I}_h^0$  with  $\mathcal{I}_h^0 f|_C = f(s_C)$ , where  $s_C$  is the center of gravity of any element  $C \in \mathcal{C}$ , and define a general weighted lumped mass matrix

$$\mathbf{M}[\omega] := \left( \int_{\Omega} \mathcal{I}_h^0(\omega) \mathcal{I}_h(\Phi_i \Phi_j) \, dx \right)_{i,j \in I}$$

Furthermore, we consider the Lagrangian projection  $\mathcal{I}_h^1$  corresponding to the four Gaussian quadrature nodes on each element, which ensure an exact integration up to third order tensor product polynomials. Based on this notation we define a weighted second order stiffness matrix

$$\mathbf{L}[\omega] := \left( \int_{\Omega} \mathcal{I}_h^1(\omega \nabla \Phi_i \cdot \nabla \Phi_j) \, dx \right)_{i,j \in I}.$$

Finally, for a discrete function  $\Phi \in V^h$  we denote by  $\bar{\Phi}$  the nodal coordinate vector and formulate the resulting fully practical version of the numerical scheme in matrix form:

We initialize  $\bar{\Phi}^0 := \overline{\mathcal{I}_h \phi_0}$  and solve in each timestep either the system of linear equations resulting from variant I

$$\mathbf{A}^I \bar{\Phi}^{k+1} = \mathbf{M} \bar{\Phi}^k$$

with

$$\begin{aligned} \mathbf{M} &:= \mathbf{M}[\|\nabla \Phi^k\|_{\epsilon}^{-1}], \\ \mathbf{A}^I &:= \mathbf{M} + \frac{\tau}{2} \mathbf{L}_1 + \tau \mathbf{L}_2 \mathbf{M}^{-1} \mathbf{L}_3, \\ \mathbf{L}_1 &:= \mathbf{L}[(W^k)^2 \|\nabla \Phi^k\|_{\epsilon}^{-3}], \\ \mathbf{L}_2 &:= \mathbf{L}[P_{\epsilon}[\Phi^k] \|\nabla \Phi^k\|_{\epsilon}^{-1}], \\ \mathbf{L}_3 &:= \mathbf{L}[\|\nabla \Phi^k\|_{\epsilon}^{-1}], \end{aligned}$$

or from variant II

$$\mathbf{A}^{II} \bar{\Phi}^{k+1} = \mathbf{M}[\|\nabla \Phi^k\|_{\epsilon}] \bar{\Phi}^k + \tau \mathbf{L}_4 \mathbf{M}^{-1} \mathbf{L}_3 \bar{\Phi}^k$$

where

$$\begin{aligned} \mathbf{A}^{II} &:= \mathbf{M} + \frac{\tau}{2} \mathbf{L}_1 + \tau \mathbf{L}_3 \mathbf{M}^{-1} \mathbf{L}_3, \\ \mathbf{L}_4 &:= \tau \mathbf{L}[(\mathbb{I} - P_{\epsilon}[\Phi^k]) \|\nabla \Phi^k\|_{\epsilon}^{-1}]. \end{aligned}$$

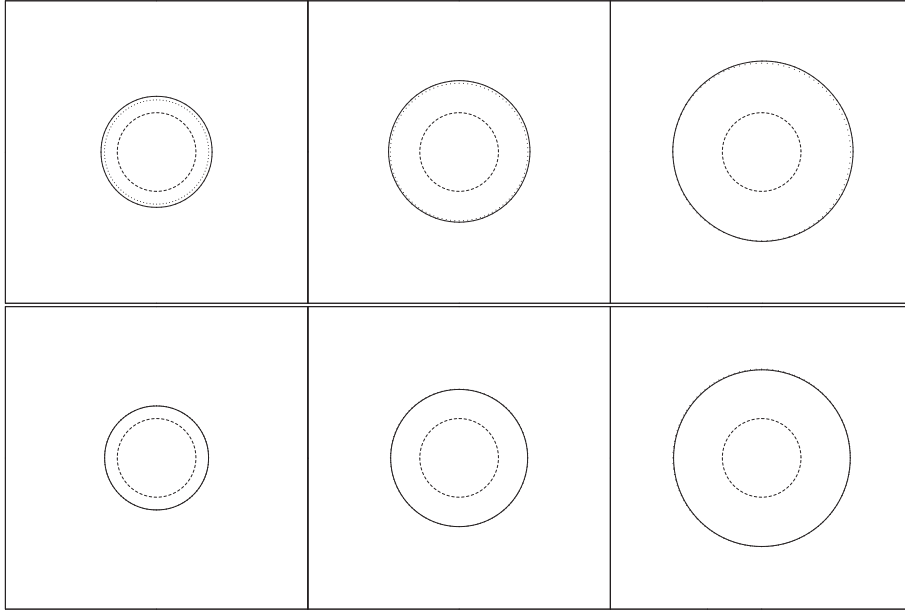


Figure 2: A circle of radius  $r_0 = 0.13$  expands due to its propagation via Willmore flow ( $h = 64^{-1}$  (top row), and  $h = 128^{-1}$  (bottom row),  $\tau = 10h^4$ ). The circle is represented by a level set function. During the evolution by the level set method for Willmore flow a signed distance function is recomputed every 50<sup>th</sup> time step. The exact solution (dotted line) and the corresponding level set (solid line) are plotted for different times  $t = 2.99 \cdot 10^{-4}$ ,  $1.192 \cdot 10^{-3}$  and  $3.576 \cdot 10^{-3}$ .

Although we did not observe any problem in the numerical simulation, the solvability of the linear system of equation appearing in variant I is still unclear. Furthermore, the linear system matrix  $\mathbf{A}^I$  is not symmetric. Thus, in the implementation we apply BiCGstab [5] as iterative solver. Concerning variant II, the corresponding matrix  $\mathbf{A}^{II}$  is obviously symmetric and positive definite. Hence,  $\mathbf{A}^{II}$  is invertible and the linear systems of equations can be solved applying a CG method.

## 9 Numerical Results

In this section we will describe numerical experiments to validate the presented algorithms for discrete Willmore flow.

At first, we consider the limit behaviour in the case of graphs.  $S^2$  is known to be a stationary surface for Willmore flow in three space dimensions. Hence, we consider as Dirichlet boundary conditions the correct positions and normals of a spherical cap,  $\phi^*(x, y) = \sqrt{r^2 - x^2 - y^2}$  for  $r = 1$ , over a rectangular domain. As initial surface graph  $\phi_0$ , we select the discrete solution of Poisson problems  $\Delta\phi = 0$  in  $\Omega$  with  $\phi_0 = \phi^*$  on  $\partial\Omega$ . Setting  $\epsilon = 1$  we compute the evolution using variant I. As expected

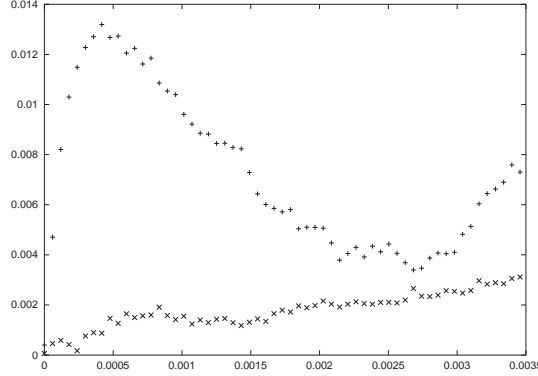


Figure 3: The error function  $\|r(t) - r(t, \cdot)\|_{L^\infty(\mathcal{M}_c(t))}$  is plotted for the numerical solutions computed on two different grids with  $h = 64^{-1}$  (marked by +) and  $h = 128^{-1}$  (marked by x), respectively.

$h$	$2^{-3}$	$2^{-4}$	$2^{-5}$	$2^{-6}$	$2^{-7}$	$2^{-8}$
$L^2$ -error	1.043e-3	2.519e-4	6.244e-5	1.575e-5	4.002e-6	1.219e-6
EOC		2.05	2.01	1.99	1.98	1.71

Table 1:  $L^2$ -error and experimental order of convergence for the limit surface of the Willmore flow which is expected to converge to a sphere cap depending on the grid size  $h$ .

and illustrated in Figure 1 we observe  $\Phi_h^k \xrightarrow{k \rightarrow \infty} \Phi_h \approx \mathcal{I}_h \phi^*$ . Here, we study the convergence behaviour depending on  $h$ , and verify  $\|\Phi_h - \mathcal{I}_h \phi^*\| \leq Ch^2$ , which reflects the order of the interpolation error (cf. Table 1).

Next, we deal with Willmore flow in the radial symmetric case in

Next, we deal with Willmore flow in the radial symmetric case in 2D. The evolution of the level sets can be described by an ordinary differential equation for the radius:  $\dot{r}(t) = \frac{1}{2}r(t)^{-3}$ . Hence, we obtain for a circle with initial radius  $r(0) = r_0$  obtain the curve evolution

$$r(t) = (2t + r_0^4)^{\frac{1}{4}}. \quad (14)$$

For a radial symmetric initial function  $\phi_0$  we compute the discrete Willmore flow with  $\epsilon = \frac{h}{2}$  on a  $65 \times 65$  and a  $129 \times 129$  grid for the domain  $\Omega = (-\frac{1}{2}, \frac{1}{2})^2$ . We track a particular level set  $\mathcal{M}_c$  and reinitialize  $\Phi^k$  every  $50^{th}$  timestep computing a signed distance function [31] with respect to  $\mathcal{M}_c$ . Figure 2 shows a comparison between the exact evolution given by  $r(t)$  from (14) and the discrete evolution. Let us emphasize that there are two sources of error: discretization errors in the actual algorithms for Willmore flow and interpolation error due to the reinitialization of the discrete signed distance function. The  $L^\infty$  error of the radius  $r(t, \cdot) : \mathcal{M}_c(t) \rightarrow \mathbb{R}$  by  $r(t, x) = |x|$  is plotted in Figure 3.

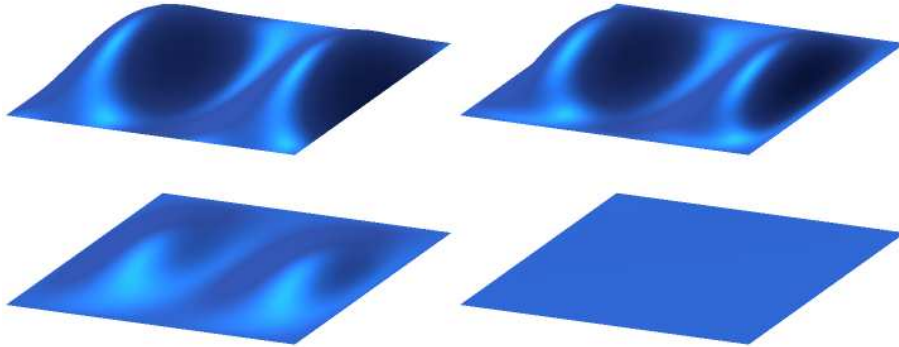


Figure 4: *Different time steps of discrete Willmore flow for graphs over the domain  $\Omega = (0, 1)^2$  (from left to right and top to bottom  $t = n10^{-8}$ ,  $n = 0, 100, 1000, 2500$ ).*

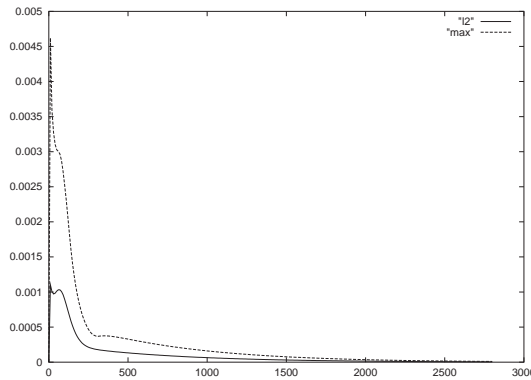


Figure 5:  *$L^2$  (solid line) and  $L^\infty$  (dashed line) difference of discrete Willmore flow for graphs and parametric surface is plotted over time.*

For a further validation of our algorithm, we compare the numerical method for the evolution of graphs under Willmore flow with a different parametric finite element method for Willmore flow presented in [10]. In this context it would be also interesting to analyze the error for both methods for comparison, but due to the lack of geometries for which the exact evolution under Willmore flow is known analytically, we analyzed the  $L^2$ -difference between the graph and the parametric surface.

As initial function we define

$$\phi_0 : [0, 1]^2 \rightarrow \mathbb{R}, (x, y) \mapsto -\frac{1}{4} \sin(\pi y) \left( \frac{1}{4} \sin(\pi x) + \frac{1}{2} \sin(3\pi x) \right)$$

and subsequently generate a triangulation of the graph as input for the parametric algorithm. Here, we use a  $65 \times 65$  grid and a time step size  $\tau = 10^{-6}$ . Different time steps of the discrete graph evolution ( $\epsilon = 1$ ) are shown in Figure 4. As Dirichlet boundary



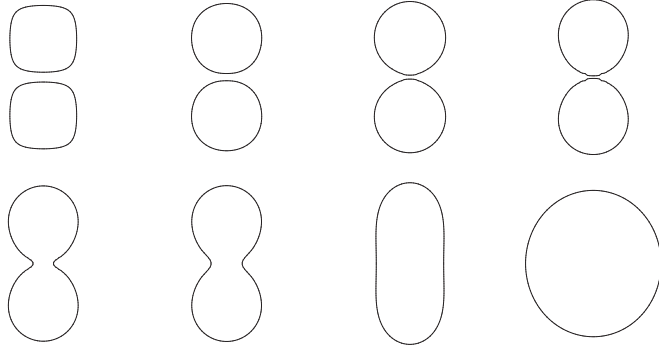


Figure 6: Two shapes merge under the level set evolution of Willmore flow. The parameters were chosen as follows:  $\epsilon = 5h$ , where  $h = 128^{-1}$ , the time step size  $\tau$  was  $10h^4$ . Timesteps 0, 100, 800, 1600, 1700, 1800, 4000, 40000 are depicted from top left to bottom right.

conditions we set  $\phi(t) = 0$  on  $\partial\Omega$  and upwards pointing normals. After converting the evolving triangulation of the discrete parametric surface back to a graph representation by Lagrangian interpolation at the grid nodes, the  $L^2$  and  $L^\infty$  difference between the two discrete solutions is plotted in Figure 5.

In Figure 6 we demonstrate a change of topology under Willmore flow. An initial configuration of two square-like shapes is first rounded off by the gradient flow until these shapes resemble circles, which then – due to the observation that small circles yield a higher energy than large circles – in turn grow outwards until the boundaries are in contact with each other, merge and eventually evolve to a single circle.

Finally, in Figure 7 an initial function with ellipse-like level sets in attached to the boundary is evolved under Willmore flow for level sets with  $\epsilon = h$  using variant II of the algorithm. The initial function is given by

$$\phi_0 : [0, 1]^2 \rightarrow \mathbb{R}, (x, y) \mapsto 1 + e^{1 - \frac{1}{1-y^2}} \cos(\pi x) \cos\left(\left(\frac{1}{2} + \frac{3}{2}(3x^2 - 2x^3)\right)\pi y\right).$$

Clearly we observe that the ellipses tend to get rounder. The applied Neumann boundary conditions ensure orthogonality of the level lines at the boundary. We additionally observe a concentration of level sets and a steepening of the gradient as well as a flattening behaviour in other regions.

The condition of the discrete operator  $\mathbf{M}^{-1}\mathbf{A}^{II}$  is dominated by the discretization of the fourth-order term  $\mathbf{M}^{-1}\mathbf{L}_3\mathbf{M}^{-1}\mathbf{L}_3$ . If the level set function is initialized as a signed distance function, i. e.,  $\|\nabla\phi\| \equiv 1$  then  $\mathbf{L}_3$  corresponds to the usual stiffness matrix and  $\mathbf{M}$  to the usual lumped mass matrix, and the condition number scales like  $h^{-4}$ . However if  $\|\nabla\phi\|$  varies in space, the condition number of  $\mathbf{M}$  and  $\mathbf{L}_3$  may be spread by a factor of  $\frac{M}{m}$ , where  $M := \sup_{\Omega} \|\nabla\phi\|$  and  $m := \inf_{\Omega} \|\nabla\phi\|$  which then leads to an even worse conditioned system, which is reflected in significantly larger numbers of CG-iterations necessary for each time step. Here variants of multilevel preconditioners may provide substantial speed-up of the linear solver.

## Acknowledgement

The authors would like to thank G. Dziuk and U. Clarenz for inspiring discussions on Willmore flow. In particular, G. Dziuk gave us the hint to look for a different dependent variable than the mean curvature, which finally lead to the new approach presented here.

## References

- [1] L. Ambrosio, N. Fusco, and D. Pallara. *Functions of bounded variation and free discontinuity problems*. Oxford University Press, 2000.
- [2] L. Ambrosio and S. Masnou. A direct variational approach to a problem arising in image reconstruction. *Interfaces Free Bound.*, 5(1):63–81, 2003.
- [3] E. Bänsch, P. Morin, and R. H. Nochetto. Finite element methods for surface diffusion. In *proceedings of the International Conference on Free Boundary Problems, Theory and Applications, Trento, Italy, 2002*.
- [4] E. Bänsch, P. Morin, and R. H. Nochetto. Surface diffusion of graphs: Variational formulation, error analysis and simulation. *SIAM Num. Anal.*, 2002. to appear.
- [5] R. Barrett, M. Berry, T. F. Chan, J. Demmel, J. Donato, J. Dongarra, V. Eijkhout, R. Pozo, C. Romine, and H. V. der Vorst. *Templates for the Solution of Linear Systems: Building Blocks for Iterative Methods, 2nd Edition*. SIAM, Philadelphia, PA, 1994.
- [6] M. Bertalmio, A. Bertozzi, and G. Sapiro. Navier-Stokes, fluid dynamics, and image and video inpainting. *Proceedings of the International Conference on Computer Vision and Pattern Recognition, IEEE*, I:355–362, 2001.
- [7] M. Bertalmio, G. Sapiro, V. Caselles, and C. Ballester. Image inpainting. In K. Akeley, editor, *Computer Graphics (SIGGRAPH '00 Proceedings)*, pages 417–424, 2000.
- [8] T. F. Chan, S. H. Kang, and J. Shen. Euler’s elastica and curvature-based inpainting. *SIAM Appl. Math.*, 63(2):564–592, 2002.
- [9] P. Ciarlet. *Mathematical Elasticity, Vol III: Theory of Shells*. North-Holland, 2000.
- [10] U. Clarenz, U. Diewald, G. Dziuk, M. Rumpf, and R. Rusu. A finite element method for surface restoration with smooth boundary conditions. *CAGD*, 2004. to appear.
- [11] K. Deckelnick and G. Dziuk. Convergence of a finite element method for non-parametric mean curvature flow. *Numer. Math.*, 72:197–222, 1995.
- [12] K. Deckelnick and G. Dziuk. Discrete anisotropic curvature flow of graphs. *Math. Modelling Numer. Anal.*, 33:1203–1222, 1999.

- [13] K. Deckelnick and G. Dziuk. Error estimates for a semi implicit fully discrete finite element scheme for mean curvature flow of graphs. *Interfaces and Free Boundaries*, 2:341–359, 2000.
- [14] K. Deckelnick and G. Dziuk. Numerical approximation of mean curvature flow of graphs and level sets. In P. Colli and J. F. Rodrigues, editors, *Mathematical Aspects of Evolving Interfaces, Madeira, Funchal, Portugal, 2000. Lecture Notes in Mathematics*, volume 1812, pages 53–87. Springer-Verlag Berlin Heidelberg, 2003.
- [15] K. Deckelnick, G. Dziuk, and C. M. Elliott. Error analysis of a semidiscrete numerical scheme for diffusion in axially symmetric surfaces. CMAIA Research Report 2002/05, University of Sussex, 2002. to appear in *SIAM J. Numer. Anal.*
- [16] G. Dziuk, E. Kuwert, and R. Schätzle. Evolution of elastic curves in  $\mathbb{R}^n$ : existence and computation. *SIAM J. Math. Anal.*, 33(5):1228–1245 (electronic), 2002.
- [17] L. Evans and J. Spruck. Motion of level sets by mean curvature I. *J. Diff. Geom.*, 33(3):635–681, 1991.
- [18] L. C. Evans and R. F. Gariepy. *Measure Theory and Fine Properties of Functions*. CRC Press, 1992.
- [19] C. Fehmi, M. Scott, E. Antonsson, M. Ortiz, and P. Schröder. Integrated modeling, finite element analysis, and engineering design for thin-shell structures using subdivision. *Computer-Aided Design*, 34(2):137–148, 2002.
- [20] E. Grinspun, P. Krysl, and P. Schröder. CHARMS: A Simple Framework for Adaptive Simulation. In *Computer Graphics (SIGGRAPH '02 Proceedings)*, 2002.
- [21] E. Kuwert and R. Schätzle. The Willmore flow with small initial energy. *J. Differential Geom.*, 57(3):409–441, 2001.
- [22] E. Kuwert and R. Schätzle. Gradient flow for the Willmore functional. *Comm. Anal. Geom.*, 10(5):1228–1245 (electronic), 2002.
- [23] E. Kuwert and R. Schätzle. Removability of Point Singularities of Willmore Surfaces. *Preprint SFB 611, Bonn*, No. 47, 2002.
- [24] S. Masnou. Disocclusion: A variational approach using level lines. *IEEE Transactions on Image Processing*, 11(2):68–76, 2002.
- [25] S. Osher and N. Paragios. *Geometric Level Set Methods in Imaging, Vision and Graphics*. Springer, 2003.
- [26] A. Polden. Closed Curves of Least Total Curvature. *SFB 382 Tübingen, Preprint*, 13:, 1995.

- [27] A. Polden. Curves and Surfaces of Least Total Curvature and Fourth-Order Flows. *Dissertation, Universität Tübingen*, page , 1996.
- [28] R. Rusu. An algorithm for the elastic flow of surfaces. *Preprint Mathematische Fakultät Freiburg*, 01-35:, 2001.
- [29] R. Schneider and L. Kobbelt. Discrete Fairing of Curves and Surfaces based on Linear Curvature Distribution. In *Curve and Surface Design: Saint-Malo*, pages 371–380, 1999.
- [30] R. Schneider and L. Kobbelt. Generating fair meshes with G1 boundary conditions. In *Geometric Modeling and Processing Conference Proceedings*, pages 251–261, 2000.
- [31] J. A. Sethian. *Level Set Methods: Evolving Interfaces in Geometry, Fluid Mechanics, Computer Vision and Materials Sciences*. Cambridge Univ. Press, 1996.
- [32] G. Simonett. The Willmore Flow near spheres. *Diff. and Integral Eq.*, 14(8):1005–1014, 2001.
- [33] V. Thomée. *Galerkin - Finite Element Methods for Parabolic Problems*. Springer, 1984.
- [34] T. Willmore. *Riemannian Geometry*. Clarendon Press, Oxford, 1993.
- [35] S. Yoshizawa and A. Belyaev. Fair Triangle Mesh Generation with Discrete Elastica. In *Geometric Modeling and Processing, RIKEN, Saitama, Japan*, pages 119–123, 2002.

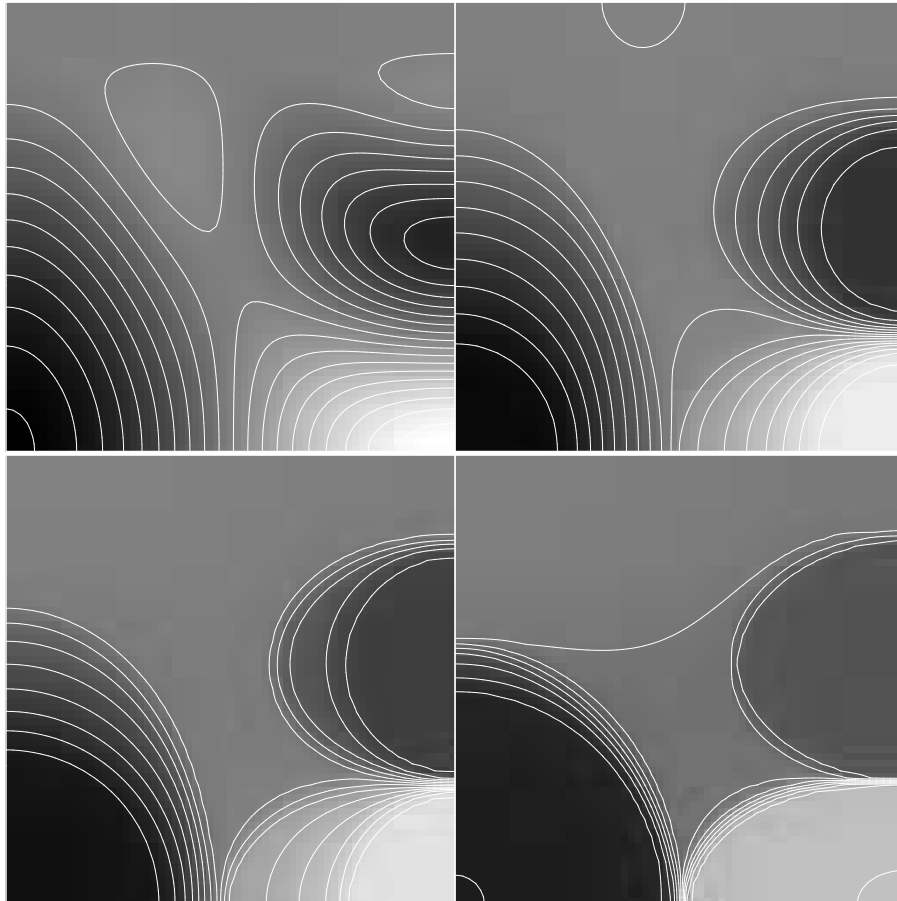


Figure 7: On the top left, some level sets of the initial configuration are shown on top of the level set function  $\phi_0$  represented by a gray scale image. From top to bottom and left to right the evolution is depicted at times  $t = 10^{-3}$ ,  $5 \cdot 10^{-3}$  and  $2.5 \cdot 10^{-2}$ .